Crystal Field Analysis and Electron-phonon Coupling in Sc_2O_3:Cr^{3+}

M. G. Brik and N. M. Avram[a]

Fukui Institute for Fundamental Chemistry, Kyoto University, 34-4 Takano Nishihiraki-cho,
Sakyo-ku, Kyoto 606-8103, Japan
[a] Department of Physics, West University of Timisoara, Bd. V. Parvan No. 4, 300223, Timisoara,
Romania

Reprint requests to Dr. M. G. B.; E-mail: brik@fukui.kyoto-u.ac.jp

Z. Naturforsch. **59a,** 799 – 803 (2004); received June 26, 2004

Crystal field analysis of the energy level structure of the Cr^{3+} ion in the Sc_2O_3 crystal is performed, using the exchange charge model of the crystal field theory. The crystal field parameters acting on the optical electrons of the Cr^{3+} ion at the sites with C_2 and C_{3i} symmetry are calculated from the crystal structure data. On the basis of the comparison between experimental absorption and emission spectra and theoretically calculated energy levels of Sc_2O_3:Cr^{3+}, the conclusion is made that the spectroscopic properties of the title host are determined by the Cr^{3+} ion at the positions of C_2 local symmetry. The Stokes shift $S = 4.32$ and the energy of the phonons effectively interacting with an impurity center $\hbar\omega = 499$ cm^{-1} are derived from the experimental spectra of absorption and emission.

Key words: Crystal Field Theory; 3*d*-ions; Electron-phonon Coupling.

1. Introduction

Crystals doped with Cr^{3+} have received considerable attention since 1960, when the first laser at all was realized with Al_2O_3:Cr^{3+} (ruby) [1]. Later on, many other crystals were shown to lase with the Cr^{3+} ion; the number of them is now about 20, and the lasers based on these hosts cover the spectral region between 700 nm and 1100 nm [2]. Such a wide tunability region is entirely due to the vibronic interaction between optical electrons of the Cr^{3+} ion and vibrations of the host lattice ions.

Very often several types of impurity centers co-exist in the same crystal, and not always it becomes possible to unambiguously distinguish between them. Thorough spectroscopic measurements or detailed crystal field calculations are needed in this case to understand the nature of an impurity center. In this paper we use the crystal field theory to analyze the energy level scheme of the octahedrally coordinated Cr^{3+} in a Sc_2O_3 crystal in which two types of Cr^{3+} positions are available, and deduce the parameters of the electron-phonon coupling from the experimental data found in the literature.

2. Crystal Structure and Spectroscopy of Sc_2O_2:Cr^{3+}

Scandiumoxide (Sc_2O_3) is a cubic crystal which belongs to the *Ia*3 space group (space group number 206) [3]. The lattice constant is 9.8459 Å, the unit cell consists of 16 formula units. Among the 32 Sc^{3+} ions in the unit cell, 8 occupy the site with the C_{3i} symmetry and 24 occupy the site with C_2 symmetry. Each Sc^{3+} ion is surrounded by six O^{2-} ions, the Cartesian coordinates of which for both types of the above mentioned positions, obtained using data from [3], are given in Tables 1 and 2.

The experimental spectroscopic data of Cr^{3+}-doped Sc_2O_3 can be found in [4, 5]. The shape of the experimental spectra is typical for octahedrally coordinated Cr^{3+} ions. Analysis of the excitation spectrum performed in [5] led to the following energy level assignment (for the spin-allowed transitions): $^4A_{2g}(^4F)$ – $^4T_{2g}(^4F)$ at 670 nm (14925 cm^{-1}), $^4A_{2g}(^4F)$ – $^4T_{1g}(^4F)$ at 480 nm (20833 cm^{-1}), $^4A_{2g}(^4F)$ – $^4T_{1g}(^4P)$ at 300 m (33333 cm^{-1}). The sharp line around 710 nm (14084 cm^{-1}) was assigned to the $^4A_{2g}(^4F)$ – $^2E_g(^2G)$ spin-forbidden transition. The broad band emission

Table 1. Cartesian coordinates (in Å) of ions of the $[CrO_6]^{9-}$ cluster in the Sc_2O_3 crystal (C_{3i} site).

Ion	*X*	*Y*	*Z*
Cr^{3+}	0	0	0
O^{2-}	−1.41092	0.97179	−1.31443
O^{2-}	−1.31443	−1.41092	0.97179
O^{2-}	0.97179	−1.31443	−1.41092
O^{2-}	1.41092	−0.97179	1.31443
O^{2-}	1.31443	1.41092	−0.97179
O^{2-}	−0.97179	1.31443	1.41092

Table 2. Cartesian coordinates (in Å) of ions of the $[CrO_6]^{9-}$ cluster in the Sc_2O_3 crystal (C_2 site).

Ion	*X*	*Y*	*Z*
Cr^{3+}	0	0	0
O^{2-}	1.49658	1.05056	0.97179
O^{2-}	1.49658	−1.05056	−0.97179
O^{2-}	−0.70103	−1.48968	1.31443
O^{2-}	−0.70103	1.48968	−1.31443
O^{2-}	−1.14016	−1.14705	−1.41092
O^{2-}	−1.14016	1.14705	1.41092

between 700 and 1100 nm, centered at around 900 nm, was assigned to the $^4T_{2g}$ (^4F) – $^4A_{2g}$(^4F) transition of the Cr^{3+} ion. The crystal field strength *Dq* and the Racah parameters *B* and *C* obtained in [5] from experimental data are (in cm^{-1}) 1490, 590, and 3227, respectively.

3. Crystal Field Calculations for Sc_2O_2:Cr^{3+}

The energy levels of Cr^{3+} ion in this work are represented by the eigenvalues of the crystal field Hamiltonian of the form [6]

$$h = \sum_{p=2,4} \sum_{k=-p}^{p} B_p^k O_p^k, \tag{1}$$

where O_p^k are the linear combinations of irreducible tensor operators acting on the angular parts of the Cr^{3+} ion wave functions, and B_p^k are the crystal field parameters containing all information about the geometrical structure of an impurity center. As formulated in [6], these parameters can be written as a sum of two terms:

$$B_p^k = B_{p.q}^k + B_{p.S}^k. \tag{2}$$

The first contribution is due to the electrostatic interaction between optical electrons of an impurity ion and ions of the crystal lattice (treated as point charges, without taking into account their electron structure), and the second one is proportional to the overlap of the wave functions of an impurity ion and ligands. In other words, this term includes all effects of the covalent bond formation and exchange interaction. Inclusion of these effects significantly improves the agreement between calculated and experimentally observed energy levels. Expressions for calculating both contributions to the crystal field parameters in case of the 3*d*-ion are as follows [6]:

$$B_{p.q}^k = -K_p^k e^2 \langle r^p \rangle \sum_i q_i \frac{V_p^k(\theta(i), \varphi(i))}{R(i)^{p+1}}, \tag{3}$$

$$B_{p.S}^k = K_p^k e^2 \frac{2(2p+1)}{5} \sum_i (G_s S_s(i)^2 + G_\sigma S_\sigma(i)^2 + \gamma_p G_\pi S_\pi(i)^2) \frac{V_p^k(\theta(i), \varphi(i))}{R(i)}. \tag{4}$$

The sums are carried out over lattice ions denoted by *i* with charges q_i; $R(i)$, $\theta(i)$, $\varphi(i)$ are the spherical coordinates of the *i*-th ion of the crystal lattice in the reference system centered at the impurity ion. The averaged values $\langle r^p \rangle$ of the *p*-th power of the impurity ion electrons coordinate can be found in [7]. The values of the numerical factors K_p^k, γ_p and expressions for the polynomials V_p^k are given in [6]. The overlap integrals between the *d*-functions of the central ion and the *p*- and *s*-functions of the ligands are denoted by S_s, S_σ, S_π (they correspond to the integrals (in $\langle lm|l'm'\rangle$ notation) $S_s = \langle d0|s0\rangle$, $S_\sigma = \langle d0|p0\rangle$, $S_\pi = \langle d1|p1\rangle$). G_s, G_σ, G_π are dimensionless adjustable parameters of the model, which are determined by the positions of the first three absorption bands. Very often they can be assumed to be equal to each other: $G_s = G_\sigma = G_\pi = G$. In this paper we use this simplified model. The advantage of the exchange charge model is that, if the *G* parameter is determined to fit the first absorption band, the other energy levels, located higher in energy, will also fit the experimental spectra fairly well.

Initially the exchange charge model has been formulated and developed for rare earth ions [6], but later on it has also been successfully applied to the transition metal ions in different hosts [8–12].

Since the second rank point charge parameters $B_{2,q}^k$ decrease not so fast as the fourth rank parameters $B_{4,q}^k$ (as $1/R^3$ and $1/R^5$, respectively), the contribution of the ligands from the second and further coordination spheres can be quite significant. To increase the accuracy in calculating the point charge contribution to the crystal field parameters, we considered a large cluster,

Parameter	C_{3i} site	C_2 site
B_2^{-2}	−8530	145
B_2^{-1}	−17059	17589
B_2^{0}	0	649
B_2^{1}	−17059	384
B_2^{2}	0	−2665
B_4^{-4}	−1777	1
B_4^{-3}	−31447	60699
B_4^{-2}	−9493	0
B_4^{-1}	6523	−3866
B_4^{0}	−2285	−2974
B_4^{1}	2970	1
B_4^{2}	0	−3640
B_4^{3}	35001	−1
B_4^{4}	−11424	−10781

Table 3. Crystal field parameters (in cm^{-1}) of octahedral Cr^{3+} in ScO_2O_3.

Table 4. Positions of energy levels (in cm^{-1}) of octahedral Cr^{3+} in Sc_2O_3.

O_h irrep. repres.	Experimental values [5]	Calculated (this work, C_2 center)		Calculated (this work, C_{3v} center)	
			Averaged		Averaged
$^4A_{2g}(^4F)$	0	0	0	0	0
		13686		13886	
$^4T_{2g}(^4F)$	14925	14374	14925		14925
		16716		15444[a]	
		18507		19965[a]	
$^4T_{1g}(^4F)$	20833	19779	21123		20552
		25084		21727	
		31485		28779	
$^4T_{1g}(^4P)$	33333	33592	33594		34033
		35706		36660[a]	

[a] Orbital doublet states.

consisting of 596 ions, namely 1 Cr^{3+}, 235 Sc^{3+}, and 360 O^{2-}. This cluster enables to take into account the contribution of ions located at distances up to 14.44 Å in the case of the C_2 impurity center and 16.15 Å in the case of the C_{3i} impurity center. For the exchange charge parameters in (4) only the nearest ligands were taken into account, since the overlap between an impurity ion and ligands from other than the first coordination sphere can be safely neglected.

Using (1) – (4), the ligand positions from Tables 1 and 2, and the gaussian radial wave functions for the Cr^{3+} and O^{2-} ions from [13], we obtained the values of the crystal field parameters given in Table 3. The crystal field Hamiltonian was diagonalized in the space of 10 wave functions of the lowest ^4F and ^4P terms of the Cr^{3+} ion. The Racah parameter B, which defines the energy gap between the two above terms, was chosen to be 590 cm^{-1} [5]. A significant reduction of this parameter in comparison to that of a free ion, $\beta = B_{\text{complex ion}}/B_{\text{free ion}} = 0.64$ (for the free Cr^{3+} ion we use the value $B = 918$ cm^{-1} [14]), known as the nephelauxetic effect, is caused by the covalency. The strong nephelauxetic effect for the Cr^{3+} ion in Sc_2O_3 indicates a high degree of covalency and serves as a firm justification of exchange charge model for the considered case. The adjustable parameter G was defined by fitting the calculated splittings to the experimental ones, and turned out to be 35.485 for the Cr^{3+} in the C_2 position and 35.120 for the Cr^{3+} ion in the C_{3i} position. The obtained energy levels are listed in Table 4, in comparison with experimental ones.

Since the absorption bands of Cr^{3+} in Sc_2O_3 are very broad and were not decomposed in [5] into individual bands, we found the averaged values of the energies for the group of states arising from the orbital triplets after they are split by the low-symmetry component of the crystal field. On the other hand, we assume that the barycenter of the group of levels arising from the same triplet in C_2 or C_{3i} symmetry corresponds to the energetical position of the same triplet in O_h symmetry. One can see from Table 4 that the energy level scheme calculated for the C_2 center agrees a bit better with experimental results than the energy level scheme for the C_{3i} center. Also the splitting of the orbital triplet states, which defines the width of the absorption and emission bands, must be analyzed. The full width at half maximum (FWHM) of the $^4T_{2g}$–$^4A_{2g}$ emission band at 300 K is about 2658 cm^{-1} [5], and the splitting of the $^4T_{2g}$ state in the C_2 symmetry is closer to that value than in the C_{3i} symmetry (3030 cm^{-1} and 1558 cm^{-1}, respectively). The FWHM of the $^4A_{2g}$–$^4T_{1g}$ (^4F) absorption band at 300 K is about 4500 cm^{-1} [5], and, again, it is better reproduced by the C_2 symmetry (6577 cm^{-1}) than by the C_{3i} symmetry (1762 cm^{-1}). Since no experimental data on the FWHM of the $^4A_{2g}$–$^4T_{1g}$ (^4P) absorption band were found in [5], we can not compare the results of our calculations directly with experimental measurements, but such a large splitting (7881 cm^{-1}) of the $^4T_{1g}$ (^4P) state in case of the C_{3i} symmetry seems significantly overestimated in comparison with the same result for the C_2 symmetry (4221 cm^{-1}) and splittings of other two orbital triplets, $^4T_{2g}$ (^4F) and $^4T_{1g}$ (^4F). This consideration leads to the conclusion that the Cr^{3+} ion preferably substitutes the Sc^{3+} ion at the positions of the C_2 symmetry.

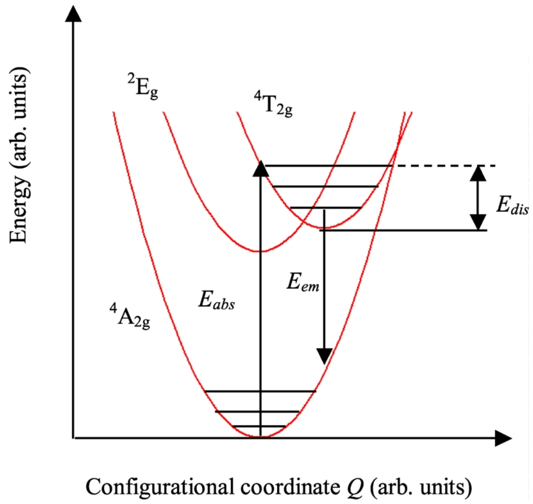

Fig. 1. Single coordinate configurational diagram for $Sc_2O_3:Cr^{3+}$ (schematic representation). The lowest electronic states are shown; the vibrational frequencies in all electronic states are assumed to be the same. Vibrational energy levels are indicated by horizontal lines. Absorption and emission transitions are indicated by the up-ward and downward arrows, respectively. The difference between the excited state vibrational level reached in the absorption transition and the minimum of the same parabola is denoted by E_{dis}.

4. Evaluation of the Parameters of Electron-phonon Interaction

To study the electron-phonon coupling of the Cr^{3+} ions with the lattice vibrations in Sc_2O_3 we used the single-coordinate configurational model in harmonic approximation [15]. This model is based on the assumption that the nearest environment of the impurity ion oscillates harmonically about its equilibrium position. This displacement is described by the Q coordinate. A typical diagram of the potential energies of electronic states as a function of the vibrational coordinate Q for the case of a strong crystal field (when the orbital doublet ^2E_g is located below the orbital triplet $^4T_{2g}$) is sketched in Figure 1.

The two main parameters which describe the electron-phonon coupling are the Huang-Rhys parameter S and the effective phonon energy $\hbar\omega$. The former is defined as the number of phonons of the energy $\hbar\omega$ excited in the absorption transition [15]:

$$S = \frac{E_{\mathrm{dis}}}{\hbar\omega} \tag{5}$$

(where E_{dis} is defined in Fig. 1). S and $\hbar\omega$ are related to the difference ΔE between the first absorption and corresponding emission band peaks [15, 16]:

$$\Delta E = (2S-1)\hbar\omega. \tag{6}$$

The second equation which is required to calculate S and $\hbar\omega$ is [15]

$$\Gamma(T) = 2.35\hbar\omega\sqrt{S\coth\left(\frac{\hbar\omega}{2kT}\right)}, \tag{7}$$

where $\Gamma(T)$ is the FWHM at the absolute temperature T. In order to solve the equations (6) and (7) we used spectroscopic data from [5]. According to these data, the energetic Stokes shift ΔE is about 3814 cm^{-1}, and $\Gamma(T)$ of the $^4T_{2g}$–$^4A_{2g}$ emission band at 300 K is about 2658 cm^{-1}. Solving (6) and (7) yields $S = 4.32$, $\hbar\omega = 499$ cm^{-1}. It is interesting to compare the obtained value of the effective phonon energy $\hbar\omega$ with the results for fluoride crystals ($\hbar\omega = 260$ cm^{-1} for $Cs_2NaAlF_6:Cr^{3+}$ [16]). The energy of the effective phonon in Sc_2O_3 is 1.9 times larger than in the fluoride. Therefore, a smaller number of phonons would be required to bridge the $^4T_{2g}$–$^4A_{2g}$ energy gap, and nonradiative quenching of the $^4T_{2g}$ state in Sc_2O_3 would be more probable than in fluorides. This conclusion is supported by measurements of the $^4T_{2g}$–$^4A_{2g}$ emission lifetime reported in [5] for $Sc_2O_3:Cr^{3+}$ (it is about 70 μs at 300 K) and in [17] for $Cs_2NaAlF_6:Cr^{3+}$ (it is significantly greater, about 180 μs at 300 K, indicating the less important role of the non-radiative processes in quenching of the excitation energy in the last case).

5. Conclusions

Calculations of the crystal field parameters and energy level structure of the octahedrally coordinated Cr^{3+} ion in Sc_2O_3 were performed in the framework of the exchange charge model of crystal field, which has only the adjustable parameter G, describing the overlap between the wave functions of the central ion and its ligands. Two possible sites – with C_2 and C_{3i} local symmetry – for the Cr^{3+} ion were considered. The positions of the energy levels and orbital triplet splittings obtained for the Cr^{3+} ion at the position with C_2 symmetry agree better with experimental spectra than those ones for the C_{3i} position. Therefore, the spectroscopic properties of the $Sc_2O_3:Cr^{3+}$ crystal are mainly determined by the Cr^{3+} ion at the positions of C_2 symmetry. The exchange charge model with its possibility of explicit inclusion of the overlap integrals into the expression for calculating the crystal field parameters provides an adequate description of the energy level scheme of Cr^{3+} in the studied crystal. The Stokes shift $S = 4.32$ and the effective phonon energy $\hbar\omega = 499$ cm^{-1} have been deduced from the experimental spectra of emission and absorption.

Acknowledgements

M. G. Brik appreciates financial support from the Japanese Ministry of Education, Culture, Sports, Science and Technology (MEXT) in a project on computational materials science unit at Kyoto University.

[1] T. H. Maiman, Nature London **187**, 493 (1960).
[2] S. Kück, Appl. Phys. B **72**, 515 (2001).
[3] O. Knop and J. M. Hartley, Canad. J. Chem. **46**, 1446 (1986).
[4] G. Huber, S. A. Payne, L. L. Chase, and W. F. Krupke, J. Lumin. **39**, 259 (1988).
[5] S. Kück, L. Fornasiero, E. Mix, and G. Huber, J. Lumin. **87-89**, 1122 (2000).
[6] B. Z. Malkin, Crystal Field and Electron-phonon Interaction in Rare-earth Ionic Paramagnets, in: A. A.Kaplyanskii and B. M. Macfarlane (Eds.), Spectroscopy of Solids Containing Rare-earth Ions, North-Holland, Amsterdam 1987, pp. 33 – 50.
[7] A. G. Abragam and B. Bleaney, Electron Paramagnetic Resonance of Transition Ions, Clarendon, Oxford 1970, chapt. 7.
[8] A. G. Avanesov, V. V. Zhorin, B. Z. Malkin, and V. F. Pisarenko, Sov. Phys. Solid State **34**, 1552 (1992).
[9] M. G. Brik, C. N. Avram, and N. M. Avram, OSA Trends in Optics and Photonics Vol. **68**, Advanced Solid-State Lasers, Martin E. Fermann and Larry R. Marshall, eds., Optical Society of America, Washington, DC 2002, pp. 275 – 279.
[10] M. G. Brik and C. N. Avram, J. Lumin. **102 – 103**, 283 (2003).
[11] C. Jousseaume, D. Vivien, A. Kahn-Harari, and B. Z. Malkin, Opt. Mater. **24**, 143 (2003).
[12] M. G. Brik, C. N. Avram, and I. Tanaka, Phys. Stat. Sol. (b) (2004) DOI 10.1002/pssb.200402041.
[13] M. V. Eremin, in: Spectroscopy of Laser Crystals (in Russian), Moscow, 1989, pp. 30 – 44.
[14] R. C. Powell, Physics of Solid-State Laser Materials, Springer, Berlin 1998.
[15] B. Henderson and G. F. Imbush, Optical Spectroscopy of Inorganic Solids, Clarendon Press, Oxford 1989.
[16] G. A. Torchia, O. Martinez-Matos, N. M. Khaidukov, and J. O. Tocho, Solid State Commun. **130**, 159 (2004).
[17] L. P. Sosman, A. D. Tavares Jr., R. J. M. da Fonseca, T. Abritta, and N. M. Khaidukov, Solid State Commun. **114**, 661 (2000).